Fermion resonances on multi-field thick branes

Fermion resonances on multi-field thick branes

Yu-Xiao Liu,[a] **Hai-Tao Li,**[a,1] **Zhen-Hua Zhao,**[a] **Jing-Xin Li**[b] **and Ji-Rong Ren**[a]

[a]*Institute of Theoretical Physics, Lanzhou University,*
Lanzhou 730000, China

[b]*College of Atmospheric Sciences, Lanzhou University,*
Lanzhou 730000, China

E-mail: liuyx@lzu.edu.cn, liht07@lzu.cn, zhaozhh02@gmail.com,
lijx08@lzu.cn, renjr@lzu.edu.cn

ABSTRACT: Motivated by the recent work on the fermion resonances on scalar-constructed thick branes (arXiv:0901.3543 and arXiv:0904.1785), we extend the idea to multi-scalar generated thick branes and complete previous work. The fermion localization and resonances on the three-field and two-field thick branes are investigated. With the Numerov method, our numerical results show that the resonance states also exist in the brane besides the single-field thick branes and the two-field thick branes in the former cases. This interesting phenomenon is related to the internal structure of the brane and the coupling of fermions and scalars. We find that the Kaluza-Klein chiral decomposition of massive fermion resonances is the parity-chiral decomposition. For the couplings $\eta\overline{\Psi}\phi^k\chi\rho\Psi$ and $\eta\overline{\Psi}\phi^k\chi\Psi$ for three-field and two-field models with odd positive k, respectively, the number of the resonant states decreases with k. This result is opposite to the one obtained in the single-field de Sitter thick brane (arXiv:0904.1785).

---

[1]Corresponding author.

JHEP10(2009)091

Contents

1   Introduction

A great deal of effort has been paid to the study of higher dimensional space-time with large extra dimensions [1–13]. Phenomenologically, the idea that our observed four-dimensional world is a brane embedded in a higher-dimensional space-time [2–4, 6, 8–10, 12, 13] opens up a route towards resolving the mass hierarchy problem and the cosmological constant problem. A first particle physics application of this idea was put forward in refs. [1, 3]. In the framework of (3+1)-dimensional brane scenarios, gravity is free to propagate in all dimensions, while all matter fields are confined to a 3-brane. In ref. [8], Arkani-Hamed, Dimopoulos, and Dvali proposed the large extra dimensions model, which lowers the energy scale of quantum gravity to $1\,\mathrm{TeV}$ by localizing the standard model fields to a 4-brane in a higher dimensional space-time. In this scenario, extra dimensions are compacted into a large volume that effectively dilutes the strength of gravity from the fundamental scale (the TeV scale) to the Planck scale. In ref. [9], Randall and Sundrum introduced a warped branewolrd model, which provides a novel solution of the gauge hierarchy problem in particle physics. Later developments suggested that the warped metric could even provide an alternative to compactification for the extra dimensions [10, 11].

In recent years, an increasing interest has been focused on the study of thick brane scenarios in higher dimensional space-time [14–24]. From a realistic point of view, a brane should have thickness. Thick brane scenarios based on gravity coupled to scalars have been

constructed. It is known that the modulus is not stable in RS warped scenario. While it can be stabilized by introducing scalar fields in the bulk [25]. These bulk scalar fields also provide us with a way of generating the brane as a domain wall (thick brane) in five dimensions. An important feature of these models is that we can obtain branes by a very natural way rather than by introducing them artificially. One can refer to a recent review article on the subject of the thick brane solutions [26].

In brane world scenarios, an important problem is localizing gravity and various bulk fields on the branes by a natural mechanism. In particular, the localization of spin $1/2$ fermions is very interesting and rich. For localizing fermions on the branes or domain walls, one needs to introduce other interactions in addition to gravity. In the last few years, localization mechanisms of fermions on a domain wall had been extensively studied [27–31]. Meanwhile, the same problem can also be discussed in other contexts such as gauge field [32, 33], supergravity [34], vortex background [35–38] and general spacetime background [39].

Usually, one examines the localization problem in the content of brane models constructed with one background scalar field. The finite discrete Kaluza-Klein (KK) modes (bound states) and a continuous gapless spectrum starting at a positive m^2 can be obtained for example in refs. [40–43]. In some brane models, the quasibound KK modes with a certain lifetime will appear [17, 44–47]. Especially, in recent work of ref. [45], the authors investigated fermions on the Bloch brane [49] constructed with two scalar fields ϕ and χ. With the simplest Yukawa coupling $\eta\overline{\Psi}\phi\chi\Psi$, the localization problem of fermions was studied. Resonances for both chiralities were found and their appearance is related to the internal structure of the Bloch brane. In ref. [46], the localization and resonance spectrum of fermions on a one-scalar generated dS thick brane were investigated. For a class of scalar-fermion couplings $\eta\overline{\Psi}\phi^k\Psi$ with positive odd integer k, some new nature about resonances were obtained. On the other hand, thick branes with two or more scalar background fields also have been constructed [48–50]. In this paper, our goal is to extend the idea of refs. [45, 46] to multi-field generated branes for refreshing the understanding of the localization and resonances of fermions in these brane models. We will consider fermions in the three-field constructed thick brane model as an explicit example. We also give a further analysis about resonances on the Bloch brane and compare the results obtained in different models.

The structure of this paper is as follows. In section 2, we review the multi-field thick brane models for spin 0 scalar fields and spin $1/2$ fermion fields. In section 3 we provide a complete investigation of the fermion localization and resonances on a three-scalar generated thick brane in detail. In section 4, we re-analysis the resonances in a Bloch brane model. Finally, our comments and conclusion are presented in section 5.

2　The multi-field thick brane models

In order to maintain the continuity of the whole work and make the background of this paper clear, in this section, we review the multi-field thick brane models. Followed the similar procedure in refs. [45, 46, 48], the field equations for scalars and fermions are obtained, especially we get the first-order equations by the superpotential.

2.1 Spin 0 scalar fields

Let us consider the 4+1 dimensional multi-field thick brane models. Specifically, we introduce n scalar background fields. The action for such a system is given by

$$S = \int d^4x dy \sqrt{-g} \left[\frac{1}{4}R - \frac{1}{2}\partial_M \phi \partial^M \phi - \frac{1}{2}\partial_M \chi \partial^M \chi - \cdots - \frac{1}{2}\partial_M \rho \partial^M \rho - V(\phi, \chi, \cdots, \rho) \right] \tag{2.1}$$

and the line-element is assumed as

$$ds^2 = g_{MN} dx^M dx^N = e^{2A}\eta_{\mu\nu} dx^\mu dx^\nu - dy^2, \tag{2.2}$$

where $g = \det(g_{MN})$, $M, N = 0, 1, 2, 3, 4$, e^{2A} is the warp factor, and y stands for the extra coordinate. The warp factor and the scalar fields are considered to be functions of y only, i.e., $A = A(y)$, $\phi = \phi(y)$, $\chi = \chi(y)$, $\cdots$, and $\rho = \rho(y)$.

The field equations generated from the action (2.1) with the ansatz (2.2) reduce to the following coupled nonlinear differential equations

$$\begin{aligned}
\phi'' &= \frac{\partial V(\phi, \chi, \cdots, \rho)}{\partial \phi} - 4A'\phi', \\
\chi'' &= \frac{\partial V(\phi, \chi, \cdots, \rho)}{\partial \chi} - 4A'\chi', \\
&\vdots \\
\rho'' &= \frac{\partial V(\phi, \chi, \cdots, \rho)}{\partial \rho} - 4A'\rho', \\
A'' &= -\frac{2}{3}(\phi'^2 + \chi'^2 + \cdots + \rho'^2), \\
A'^2 &= \frac{1}{6}(\phi'^2 + \chi'^2 + \cdots + \rho'^2) - \frac{1}{3}V(\phi, \chi, \cdots, \rho).
\end{aligned} \tag{2.3}$$

We suppose that the n-field models are defined by the potential

$$V(\phi, \chi, \cdots, \rho) = \frac{1}{8}\left[\left(\frac{\partial W}{\partial \phi}\right)^2 + \left(\frac{\partial W}{\partial \chi}\right)^2 + \cdots + \left(\frac{\partial W}{\partial \rho}\right)^2 \right] - \frac{1}{3}W^2, \tag{2.4}$$

where $W = W(\phi, \chi, \cdots, \rho)$ is the superpotential, which leads to the following first-order equations that solve the second order equations (2.3):

$$\phi' = \frac{1}{2}\frac{\partial W}{\partial \phi}, \qquad \chi' = \frac{1}{2}\frac{\partial W}{\partial \chi}, \qquad \cdots, \rho' \quad = \frac{1}{2}\frac{\partial W}{\partial \rho}, A' \quad = -\frac{1}{3}W. \tag{2.5}$$

2.2 Spin 1/2 fermion fields

In this subsection, we are ready to investigate whether spin half fermions can be localized on the brane. Let us consider n real scalars coupled to a massless bulk fermion by means of a general Yukawa coupling in five dimension. The starting action reads

$$S_{1/2} = \int d^5x \sqrt{-g} \left[\bar{\Psi}\Gamma^M D_M \Psi - \eta \bar{\Psi} F(\phi, \chi, \cdots, \rho)\Psi \right], \tag{2.6}$$

where the spin connection $\omega_M^{\bar{M}\bar{N}}$ in the covariant derivative

$$D_M\Psi = (\partial_M + \omega_M)\Psi = \left(\partial_M + \frac{1}{4}\omega_M^{\bar{M}\bar{N}}\Gamma_{\bar{M}}\Gamma_{\bar{N}}\right)\Psi \tag{2.7}$$

is defined as

$$\omega_M^{\bar{M}\bar{N}} = \frac{1}{2}E^{N\bar{M}}(\partial_M E_N^{\bar{N}} - \partial_N E_M^{\bar{N}}) - \frac{1}{2}E^{N\bar{N}}(\partial_M E_N^{\bar{M}} - \partial_N E_M^{\bar{M}})$$
$$-\frac{1}{2}E^{P\bar{M}}E^{Q\bar{N}}E_M^{\bar{R}}(\partial_P E_{Q\bar{R}} - \partial_Q E_{P\bar{R}}). \tag{2.8}$$

In five-dimensional space-time, fermions are four component spinors and their Dirac structure is determined by $\Gamma^M = E_{\bar{M}}^M \Gamma^{\bar{M}}$ with the E_M^M being the vielbein and $\{\Gamma^M, \Gamma^N\} = 2g^{MN}$. The indices of five-dimensional spacetime coordinates and the local lorentz indices are labelled with capital Latin letters $M, N, \ldots$ and $\bar{M}, \bar{N}, \ldots$, respectively. Γ^M are the curved gamma matrices and $\gamma^{\bar{M}}$ are the flat ones.

Following, we will derive the Schrödinger equation for the KK modes of fermions. In order to get the corresponding mass-independent potential, we perform the coordinate transformation

$$dz = e^{-A(y)}dy \tag{2.9}$$

to get a conformally flat metric

$$ds_5^2 = e^{2A(z)}(\eta_{\mu\nu}dx^\mu dx^\nu + dz^2). \tag{2.10}$$

With the metric (2.10), the nonvanishing components of the spin connection ω_M are calculated as

$$\omega_\mu = \frac{1}{2}(\partial_z A)\gamma_\mu\gamma_5. \tag{2.11}$$

Then the five-dimensional Dirac equation is read as

$$\left[\gamma^\mu\partial_\mu + \gamma^5(\partial_z + 2\partial_z A) - \eta e^A F(\phi, \chi, \rho)\right]\Psi = 0, \tag{2.12}$$

where $\gamma^\mu\partial_\mu$ is the Dirac operator on the brane.

We are now ready to study the above Dirac equation for five-dimensional fluctuations, and write the fermion field Ψ in terms of four-dimensional effective fields. Following [31], we have the general chiral decomposition

$$\Psi(x, z) = e^{-2A}\left(\sum_n \psi_{Ln}(x)f_{Ln}(z) + \sum_n \psi_{Rn}(x)f_{Rn}(z)\right), \tag{2.13}$$

where $\psi_{Ln}(x) = -\gamma^5\psi_{Ln}(x)$ and $\psi_{Rn}(x) = \gamma^5\psi_{Rn}(x)$ are the left-handed and right-handed components of a four-dimensional Dirac fermion fields, respectively, and they satisfy the four-dimensional massive Dirac equations $\gamma^\mu\partial_\mu\psi_{Ln}(x) = m_n\psi_{Rn}(x)$ and $\gamma^\mu\partial_\mu\psi_{Rn}(x) = m_n\psi_{Ln}(x)$. The KK modes $f_{Ln}(z)$ and $f_{Rn}(z)$ of the chiral decomposition of the spinor satisfy the following coupled equations

$$\left[\partial_z + \eta e^A F(\phi, \chi, \rho)\right]f_{Ln}(z) = m_n f_{Rn}(z), \tag{2.14}$$
$$\left[\partial_z - \eta e^A F(\phi, \chi, \rho)\right]f_{Rn}(z) = -m_n f_{Ln}(z). \tag{2.15}$$

In order to obtain the standard four-dimensional action for the massive chiral fermions, we need the following orthonormality conditions for $f_{Ln}(z)$ and $f_{Rn}(z)$:

$$\int_{-\infty}^{+\infty} f_{Lm}f_{Ln}dz = \int_{-\infty}^{+\infty} f_{Rm}f_{Rn}dz = \delta_{mn}, \qquad \int_{-\infty}^{+\infty} f_{Lm}f_{Rn}dz = 0. \tag{2.16}$$

With eqs. (2.14) and (2.15), we have

$$\left(\frac{d}{dz} - \eta e^A F(\phi,\chi,\rho)\right)\left(\frac{d}{dz} + \eta e^A F(\phi,\chi,\rho)\right)f_L = -m_n^2 f_L, \tag{2.17}$$

$$\left(\frac{d}{dz} + \eta e^A F(\phi,\chi,\rho)\right)\left(\frac{d}{dz} - \eta e^A F(\phi,\chi,\rho)\right)f_R = -m_n^2 f_R. \tag{2.18}$$

Hence, we get the Schrödinger-like equations for the left- and right-chiral fermions [45, 46]

$$H_L f_L(z) = m^2 f_L(z), \tag{2.19}$$

$$H_R f_R(z) = m^2 f_R(z), \tag{2.20}$$

with the corresponding Hamiltonians

$$H_L = \left(-\frac{d}{dz} + \eta e^A F(\phi,\chi,\rho)\right)\left(\frac{d}{dz} + \eta e^A F(\phi,\chi,\rho)\right), \tag{2.21}$$

$$H_R = \left(-\frac{d}{dz} - \eta e^A F(\phi,\chi,\rho)\right)\left(\frac{d}{dz} - \eta e^A F(\phi,\chi,\rho)\right). \tag{2.22}$$

The Schrödinger equations can be expressed as

$$\left[-\partial_z^2 + V_L(z)\right]f_L = m^2 f_L, \tag{2.23a}$$

$$\left[-\partial_z^2 + V_R(z)\right]f_R = m^2 f_R, \tag{2.23b}$$

where the effective Schrödinger-like potentials for the KK modes $f_{L,R}$ are

$$V_L(z) = \eta^2 e^{2A} F^2(\phi,\chi,\rho) - \eta e^A \partial_z F(\phi,\chi,\rho) - \eta e^A (\partial_z A)F(\phi,\chi,\rho), \tag{2.24a}$$

$$V_R(z) = \eta^2 e^{2A} F^2(\phi,\chi,\rho) + \eta e^A \partial_z F(\phi,\chi,\rho) + \eta e^A (\partial_z A)F(\phi,\chi,\rho). \tag{2.24b}$$

3 Fermion localization and resonances on a three-field thick brane

Let us now investigate the three-field brane models. As a natural extension of the single-field and two-field scenarios, the superpotential with three-fields could be

$$W(\phi,\chi,\rho) = 2\left(\phi - \frac{1}{3}\phi^3 - a\phi\left(\chi^2 + \rho^2\right)\right), \tag{3.1}$$

which was considered in refs. [48, 51]. Here a is a real parameter. In this case, the corresponding potential (2.4) is

$$V = \frac{1}{2}\left[4a^2\phi^2(\rho^2 + \chi^2) + \left[1 - \phi^2 + a(\rho^2 + \chi^2)\right]^2\right] - \frac{4}{3}\left[\phi - \frac{1}{3}\phi^3 - a\phi(\chi^2 + \rho^2)\right]^2. \tag{3.2}$$

The first order equations are

$$\frac{d\phi}{dy} = 1 - \phi^2 - a\left(\chi^2 + \rho^2\right), \tag{3.3a}$$

$$\frac{d\chi}{dy} = -2a\phi\chi, \tag{3.3b}$$

$$\frac{d\rho}{dy} = -2a\phi\rho, \tag{3.3c}$$

$$\frac{dA}{dy} = -\frac{2}{3}\left(\phi - \frac{1}{3}\phi^3 - a\phi\left(\chi^2 + \rho^2\right)\right). \tag{3.3d}$$

The solutions are given by

$$\phi(y) = \tanh(2ay), \tag{3.4a}$$

$$\chi(y) = \pm\sqrt{\frac{1}{a} - 2}\,\cos\theta\,\operatorname{sech}(2ay), \tag{3.4b}$$

$$\rho(y) = \pm\sqrt{\frac{1}{a} - 2}\,\sin\theta\,\operatorname{sech}(2ay), \tag{3.4c}$$

$$A(y) = \frac{1}{9a}\left[(1 - 3a)\tanh^2(2ay) - 2\ln\cosh(2ay)\right], \tag{3.4d}$$

where $0 < a < 1/2$ and $\theta \in [0, 2\pi)$. The shapes of the solutions are plotted in figure 1. It can be seen that the scalar $\phi(y)$ is a kink while $\chi(y)$ and $\rho(y)$ are campanulate. The warp factor has a normal shape and the brane thickness decreases with a. We note that the warp factor here is the same with the one in two-field thick brane case in refs. [45, 49] but different from the single-field one in refs. [19, 46]. In this paper, we take $\theta = \pi/6$ and consider the positive solutions of $\chi(y)$ and $\rho(y)$.

Now, we turn to the z-coordinate according to eq. (2.9). For general value of a, the expression of $A(y)$ (3.4d) cannot be integrated in a known explicit form. Even for the particular case $a = 1/3$, for which we have an analytical expression of $z(y)$, it is hard to get an expression for the inverse $y(z)$ in an explicit form in terms of some analytical functions, so some numerical methods are needed. The numerical result for $z(y)$ is depicted in figure 2. The derivatives with respect to z, can be calculated as a function of y by using the coordinate transformation (2.9)

$$\frac{dA(z)}{dz} = \frac{dA(y)}{dy}\frac{dy}{dz} = \frac{dA}{dy}e^{A(y)}, \tag{3.5}$$

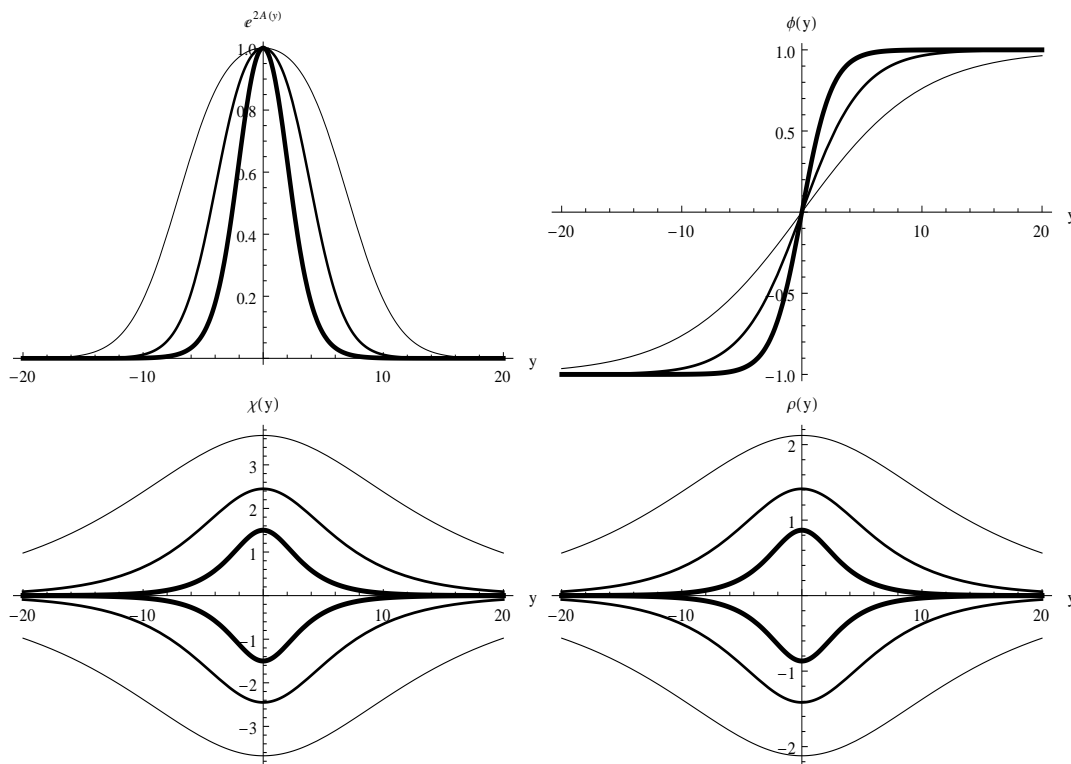$$\frac{dF(z)}{dz} = \frac{dF(y)}{dy}\frac{dy}{dz} = \frac{dF(y)}{dy}e^{A(y)}. \tag{3.6}$$

With the above expressions, we can rewrite the potentials (2.24) as a function of y:

$$V_L(z(y)) = \eta e^{2A}\left[\eta F^2(\phi, \chi, \rho) - \partial_y F(\phi, \chi, \rho) - F(\phi, \chi, \rho)\partial_y A(y)\right], \tag{3.7a}$$

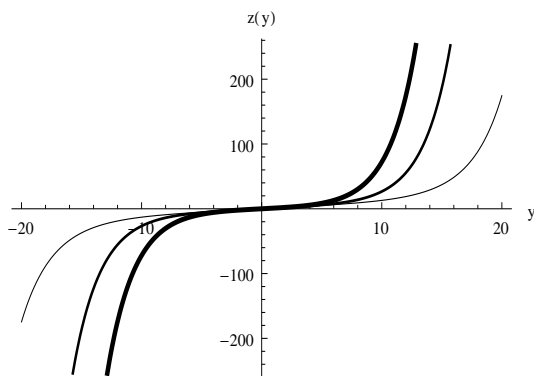$$V_R(z(y)) = V_L(z(y))|_{\eta \to -\eta}. \tag{3.7b}$$

It can be seen that, for the left- or right-chiral fermion localization, there must be some kind of scalar-fermion coupling. In addition, for the kink configuration of the scalar $\phi(y)$ and the

Figure 1. Warp factor $e^{2A(y)}$, scalar fields $\phi(y)$, $\chi(y)$ and $\rho(y)$. The parameters are set to $\theta = \pi/6$, $a = 0.05$ (thin trace), 0.1, 0.2 (thick trace). The thickness of lines is increases with a.

Figure 2. Plot of the function $z(y)$ for $a = 0.05$, 0.1 and 0.2. The thickness of lines is increases with a.

lump configurations of $\chi(y)$ and $\rho(y)$, $F(\phi, \chi, \rho)$ should be an odd function of $\phi(y)$ when one demands that $V_L(z(y))$ or $V_R(z(y))$ is Z_2-even with respect to y. Here, we would like to consider two cases: the simplest Yukawa coupling $F(\phi, \chi, \rho) = \phi\chi\rho$ and the general coupling $F(\phi) = \phi^k \chi \rho$ with odd positive k. Surely, other more complex cases can be investigated.

3.1 Case I: $F(\phi, \chi, \rho) = \phi^k \chi \rho$ with $k = 1$

Firstly, we investigate the simplest Yukawa coupling $F(\phi, \chi, \rho) = \phi\chi\rho$ for the three-scalar generated thick branes. For simplicity, we consider the brane solution (3.4) only. The explicit forms of the potentials (3.7) are given by

$$
V_L(y) = \frac{1}{288a^2}\left[\eta(2a-1)\exp\left(\frac{2(1-3a)}{9a}\tanh^2(2ay)\right)\cosh^{-6-4/(9a)}(2ay)\right]
$$
$$
\times\left[3\left(52\sqrt{3}a^2 + 9\eta - 2a(2\sqrt{3}+9\eta)\right) - 4\sqrt{3}(1+9a)\cosh(8ay)\right.
$$
$$
\left. +\left(16\sqrt{3}a + 24\sqrt{3}a^2 - 27\eta + 54a\eta\right)\cosh(4ay)\right],
$$

$$
V_R(y) = V_L(y)|_{\eta \to -\eta}. \tag{3.8b}
$$

Here, we note that y cannot be expressed in an explicit form in terms of z, so the potentials are expressed with the variable y. From figure 2, we can easily obtain the asymptotic behavior of the potentials (3.8). The values of the potentials at $z = y = 0$ and y or $z \to \pm\infty$ are given by

$$
V_L(0) = -\frac{\sqrt{3}}{2}(1-2a)\eta = -V_R(0), \tag{3.9}
$$
$$
V_L(\pm\infty) = 0 = V_R(\pm\infty). \tag{3.10}
$$

It can be seen that both potentials have the same asymptotic behavior when $z \to \pm\infty$, but opposite behavior at the origin $z = 0$, which results in the well-known conclusion: only one of the massless left- and right-chiral fermions could be localized on the brane.

As mentioned above, with the numerical methods, we can get the shape of potential function graphics as shown in figure 3. Clearly, for any value of $0 < a < 1/2$ and $\eta > 0$, $V_L(z)$ is a volcano type of potential. Therefore, the potential of the left-handed fermions does not provide mass gap between the zero-mode and KK excitation modes, and there is a continuous gapless spectrum of KK excitation modes. The zero mode of the left-handed fermions is turned out to be

$$
f_{L0}(z) \propto \exp\left(-\eta\int_0^z d\bar{z}\, e^{A(\bar{z})}\phi(\bar{z})\chi(\bar{z})\rho(\bar{z})\right)
$$
$$
= \exp\left(-\eta\int_0^y d\bar{y}\, \phi(\bar{y})\chi(\bar{y})\rho(\bar{y})\right) \tag{3.11}
$$

and the normalization condition

$$
\int_{-\infty}^{\infty} f_{L0}^2(z)dz = \int_{-\infty}^{\infty} f_{L0}^2(y)e^{-A(y)}dy
$$
$$
\propto \int_{-\infty}^{\infty}\exp\left(-A(y) - 2\eta\int_0^y d\bar{y}\,\phi(\bar{y})\chi(\bar{y})\rho(\bar{y})\right)dy
$$
$$
= \int_{-\infty}^{\infty}\exp\left(-A(y) - 2\eta\frac{3(1-2a)}{16a^2}\tanh^2(2ay)\right)dy < \infty \tag{3.12}
$$

cannot be satisfied because $A(y) \to -\frac{4}{9}y$ while $\tanh^2(2ay) \to 1$ when $y \to \infty$. Hence, the zero mode (3.12) is nonnormalizable. The reason is that the coupling $F(\phi, \chi, \rho)$ contains the
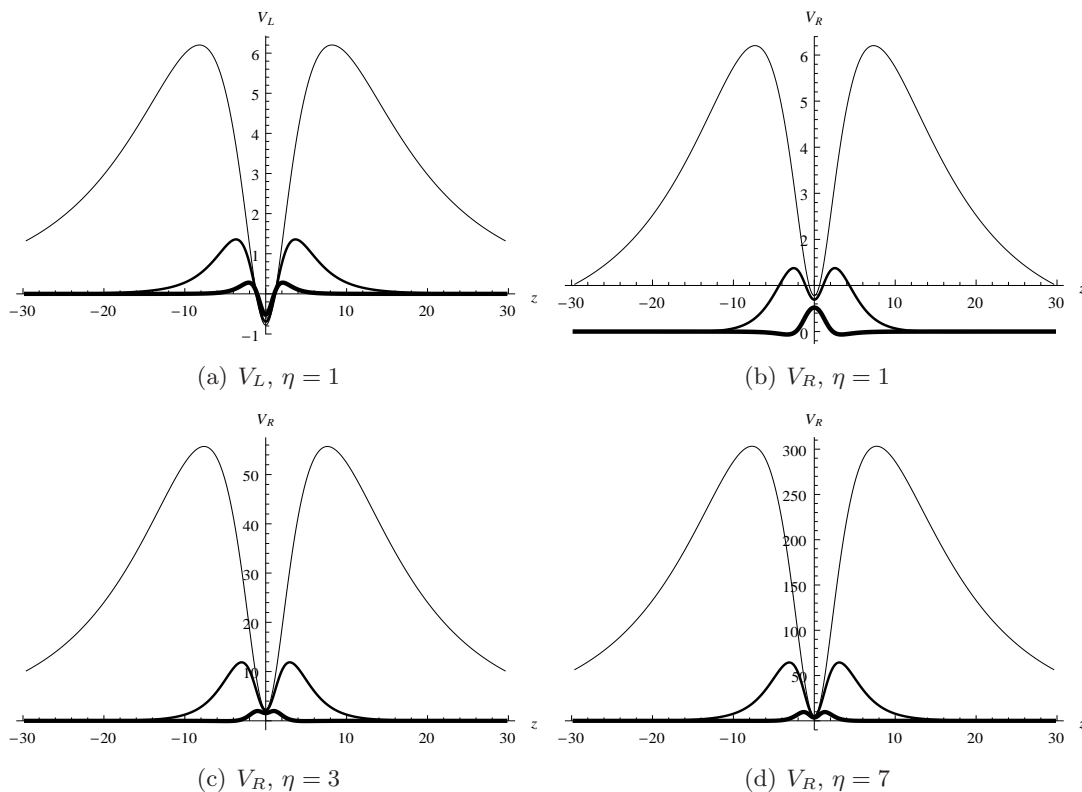
Figure 3. Potentials $V_L(z)$ and $V_R(z)$ for left- and right-chiral fermions with $F(\phi, \chi, \rho) = \phi\chi\rho$. The parameter a is set to 0.05 (thin trace), 0.1, 0.2 (thick trace).

lump configurations χ and ρ. In order to get localized zero mode for left-handed fermions, we can only consider the coupling of fermions and the kink ϕ, i.e., $F(\phi, \chi, \rho) = \phi$, for which the zero mode is normalizable provided $\eta > 2/9$. In this paper, we would not consider the special case. On the other hand, the potential $V_R(y)$ at the brane location is always positive, and when far away from the brane it gradually becomes zero. We know that this type of potential cannot trap any bound state fermions with right-chirality and there exists no zero mode of right-handed fermions. As is well known this result is consistent with the previous well-known conclusion that massless fermions must be single-handed chirality in the brane world models [27, 46].

However, the structure of the potential V_R is determined by the coupling constant η and parameter a jointly. For a given a, as η increases, there will be a potential well and the depth of the well will be deeper and deeper. On the other hand, for a given η, the smaller the parameter a is, the deeper the depth of the potential well. There is a fine-tuning relationship between a and η. This means that a competition between a and η exists. We consider the situation of the extreme one. As a range from 0 to $1/2$, for a value a which is close to $1/2$, in order to produce a potential well, we need very large η, i.e., the scalar and fermion have a strong coupling. All we can do is to find the essence of the phenomenon behind. This is the most interesting things and phenomena.

3.1.1 Left-handed fermions

We will find the following fact that the emergence of the potential wells is closely related to the resonance states, which are massive fermions with finite lifetime. A similar phenomenon for left- and right-chiral fermions can be found in refs. [45, 46], the former is in the context of two-scalar constructed thick brane with internal structure, the latter is in the background of the single-scalar generated dS thick brane with a class of scalar-fermion coupling. Here, we extend this point of view and method to a three-scalar generated thick brane obtained in ref. [48]. We follow refs. [45, 46] through solving numerically the equations (2.23) with numerical Schrödinger potentials in (3.8) to study the massive modes of fermions. In particular, in order to obtain the probability of massive modes of the fermions on the brane, we adopt the new method of calculating the probability in ref. [46]. In addition, our results are consistent with the previous two models, and some new properties about resonances are discovered.

In order to get the solutions of the KK modes $f_{L,R}(z)$ from the second order ordinary differential equations (2.23), we need additional two types of initial conditions:

$$f(0) = c_0, \qquad f'(0) = 0\,, \tag{3.13}$$

and

$$f(0) = 0, \qquad f'(0) = c_1\,. \tag{3.14}$$

From figure 3, we can see that the potentials which we will consider have even-parity. According to the knowledge of quantum mechanics, we can know that the wave functions of a Schrödinger equation with a finite smooth potential are continuous at any position. The above two types of initial conditions will lead to even-parity and odd-parity KK modes, respectively. It is worth noting that, according to a specific numerical procedure, the form of the initial conditions of equivalent deformation will be used in our followed numerical calculations. The constants c_0 and c_1 for the nonbound massive KK modes are arbitrary, and in accordance with specific conditions of numerical calculations.

From the point of view of quantum mechanics, as the general effects of the quantum mechanics, there will be tunneling effect when the massive KK modes experience the potential barrier near the brane. By means of Numerov method [52, 53], for a given potential function combined with the Schrödinger equations, the numerical results show that the corresponding KK modes with a series of masses and lifetimes will be obtained. The KK modes with finite lifetime are also called resonances, i.e., quasibound states or metastable states. Some even-parity massive KK modes of left-handed chiral fermions for the coupling $F(\phi, \chi, \rho) = \phi\chi\rho$ with different m^2 are depicted in figure 4. These graphics indicate that there are some resonance states when the mass accesses to certain specific values. The results we get here are consistent with that given in ref. [45, 46]. However, there are some new characteristics. With different models and coupling mechanisms, some new properties of resonances and physical meaning may exist. In what follows, we will carefully discuss the resonance problem in the background of the three-scalar constructed thick brane.

From figure 4, we see that, to obtain a very clear resonance, one need a very good accuracy for the parameter m^2. If we want to search for a resonance directly through
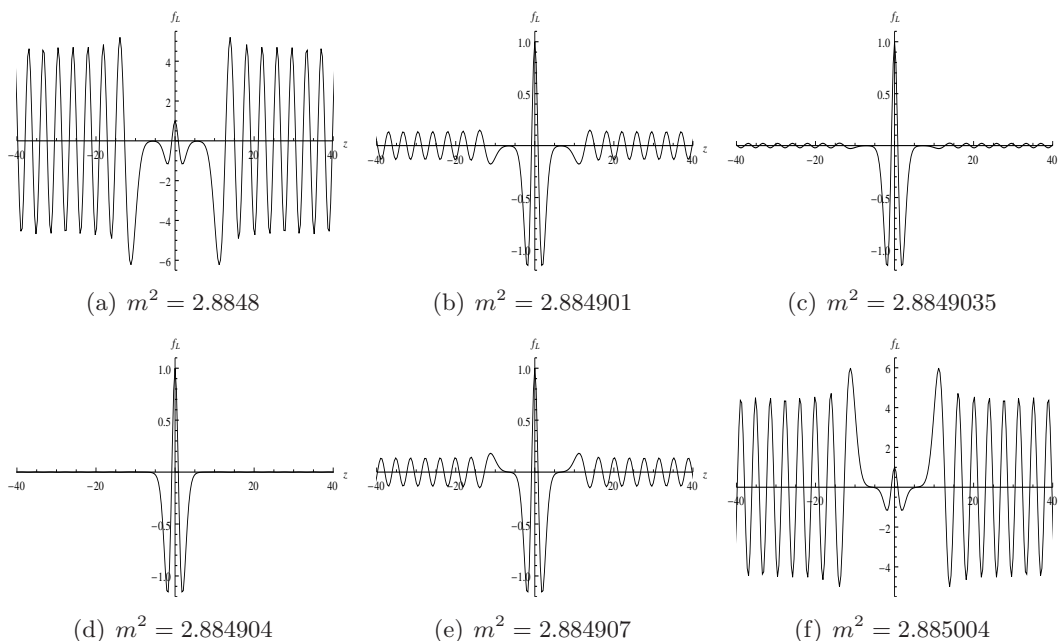
Figure 4. The shapes of the even parity massive KK modes $f_L(z)$ of left-chiral fermions for the coupling $F(\phi, \chi, \rho) = \phi\chi\rho$ with different m^2. The parameters are set to $z_{\max} = 210$, $a = 0.05$ and $\eta = 1$.

the eigenfunction and energy eigenvalue, we will encounter great difficulties and workload. According to the formal theory of resonance of quantum wave functions, we can study the probability of finding the massive KK modes around the vicinity of the brane location within a relatively large region [45, 46].

Because the formula (2.23) can be re-written in the form $\mathcal{O}_{L,R}^\dagger \mathcal{O}_{L,R} f_{L,R}(z) = m^2 f_{L,R}(z)$, so $|f_{L,R}(z)|^2$ can be interpreted as the probability for finding the massive KK modes at the position z along extra dimension. In ref. [45], the authors suggested that large peaks in the distribution of $f_{L,R}(0)$ as a function of m would reveal the existence of resonance states. Here, we follow the procedures of the extended idea in ref. [46] for the two types of initial conditions (3.13) and (3.14). For a given eigenvalue m^2, the corresponding relative probability is defined as [46]:

$$P_{L,R}(m) = \frac{\int_{-z_b}^{z_b} |f_{L,R}(z)|^2 dz}{\int_{-z_{\max}}^{z_{\max}} |f_{L,R}(z)|^2 dz}, \tag{3.15}$$

where the relation of z_b and $z_{\max}$ is selected as $z_{\max}/z_b = 10$, for which, the probability for a plane wave mode with mass m is 0.1. For the KK modes with eigenvalue m^2 much larger than the maximum of the corresponding potential function, they will have a very good plane wave approximation, and the corresponding probability $P(m)$ will tend to 0.1. For the parameters $k = 1$, $a = 0.05$, $\eta = 1$, the potential wells distribute in the range $[-z_b, z_b](z_b = 21)$ along extra dimension, so we choose $z_{\max} = 210$, and the corresponding graphics of the resonance spectra are depicted in figure 5. For left-handed fermions, we find a total of five clear resonant peaks with approximate eigenvalues $m^2 = 1.50234155$, 2.884904, 4.12957, 5.2035, 6.032. The corresponding left-handed eigenfunctions are shown
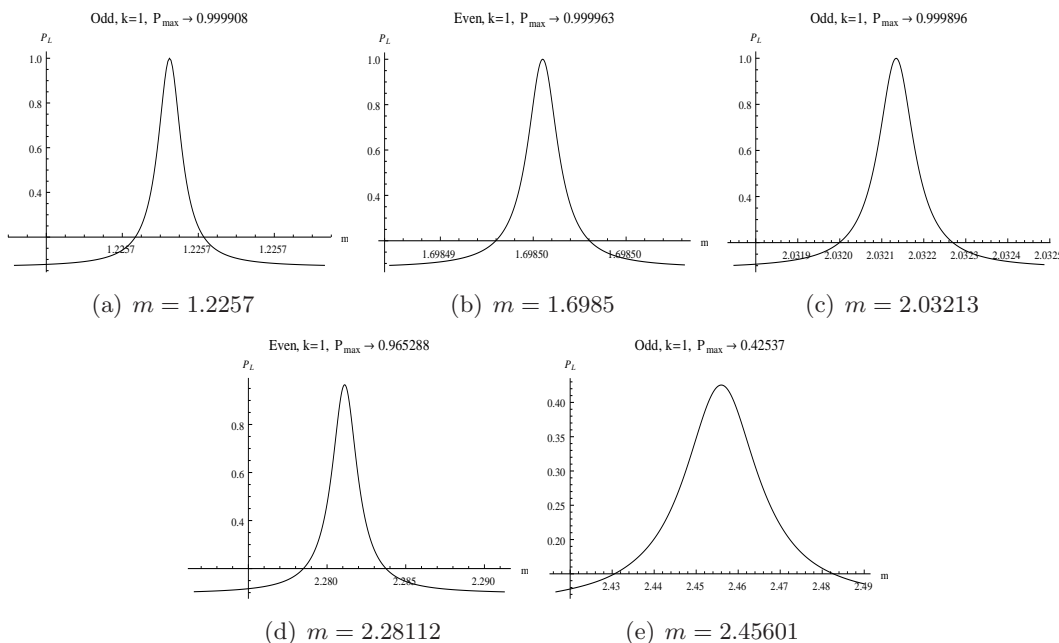
Figure 5. The probability P_L (as a function of m) for finding the even parity (under three resonant peaks) and odd parity (upper three resonant peaks) massive KK modes of left-chiral fermions around the brane location for the coupling $F(\phi, \chi, \rho) = \phi\chi\rho$. The parameters are set to $z_{\max} = 210$, $a = 0.05$ and $\eta = 1$.

in figure 6. It can be seen that the configurations of figures 6(a), 6(c) and 6(e) are odd-parity eigenfunctions, and the other two are even-parity ones. From figures 5 and 6, we can see that odd-parity eigenfunctions and even-parity eigenfunctions are placed at the five resonant peaks with irregular intervals of mass eigenvalues.

As mentioned above, it is usual to describe the resonance by its width $\Gamma = \Delta m$ at half-maximum of the corresponding resonant peak [45]. In this way, we can calculate the lifetime τ of a resonance state with the width Γ. This means that the massive fermions disappeared along the direction of extra dimension after time $\tau = 1/\Gamma$ [54]. The eigenvalues m^2, mass m, width Γ and lifetime τ for resonances of left-handed fermions corresponding to the resonant peaks shown in figure 5 are listed in table 1. We can see that the resonance states with relatively larger eigenvalues have a relatively smaller lifetimes.

In addition, it should be noted that the solutions we obtain with numerical methods are some approximate solutions which meet a certain accuracy. For example, for the even-parity resonance states shown in figure 5(d), when the step accuracy of the mass m accesses to a certain value, the fluctuation of the probability likes a hedgehog would emerge around the corresponding resonant peak (see figure 7). The overall profile of the probability fluctuation still corresponds to the resonant peak.

3.1.2 Right-handed fermions

For right-handed fermions, as we mentioned earlier, there is no normalized zero-mode. Repeating the analysis of the previous subsection, we can get the similar results about
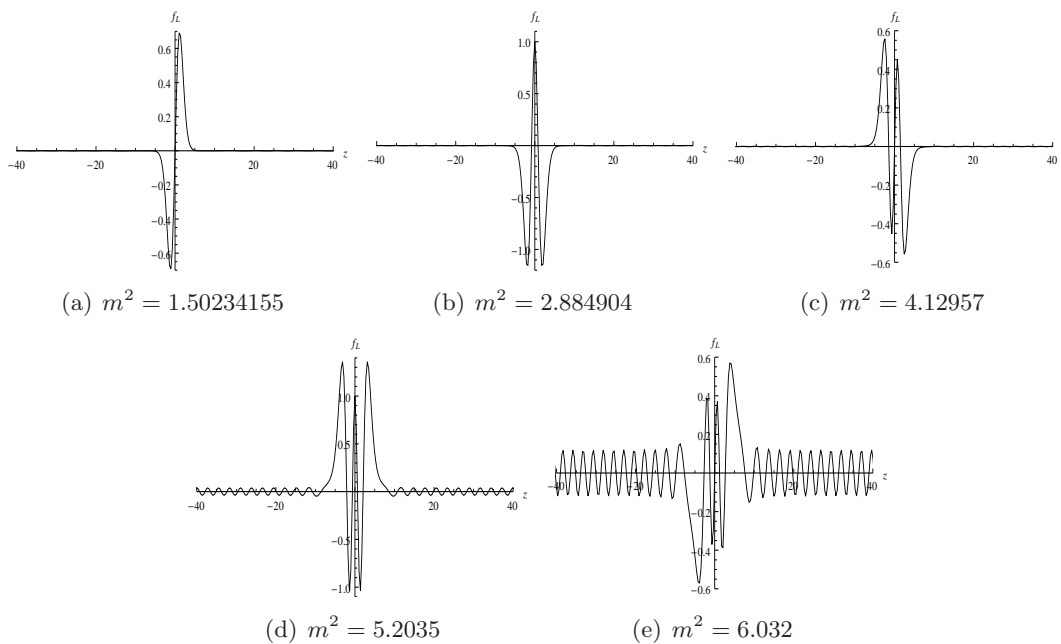
Figure 6. The shapes of the even parity and odd parity massive KK modes $f_L(z)$ of left-chiral fermions for the coupling $F(\phi, \chi, \rho) = \phi\chi\rho$ with different m^2. The parameters are set to $z_{\max} = 210$, $a = 0.05$ and $\eta = 1$.
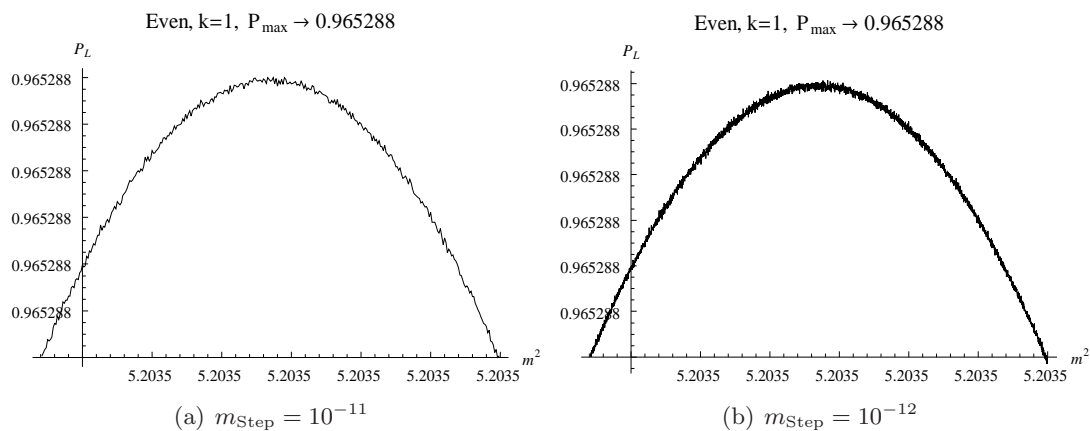
Figure 7. The fluctuation of the probability P_L (as a function of m) for finding the even parity massive KK modes of left-chiral fermions around the brane location for the coupling $F(\phi, \chi, \rho) = \phi\chi\rho$ with different step accuracy m_{Step} in numerical method. The parameters are set to $a = 0.05$ and $\eta = 1$.

resonances. And the resonance states are closely related to the emergence of the potential well shown in figure 3. For the parameters $a = 0.05$ and $\eta = 1$, the corresponding graphics of the resonance spectra are depicted in figure 8. For right-handed fermions, we also find a total of five clear resonant peaks with approximate eigenvalues $m^2 = 1.502620398$,

k	$\mathcal{C}$	$\mathcal{P}$	m_n^2	m_n	Γ	τ	$P_{\max}$
1	$\mathcal{L}$	odd	1.50234155	1.2257	7.92943×10^{-9}	1.26112×10^8	0.999908
		even	2.884904	1.6985	2.14302×10^{-6}	466631	0.999963
		odd	4.12957	2.03213	0.00011232	8903.15	0.999896
		even	5.2035	2.28112	0.00217082	460.655	0.965288
		odd	6.03	2.45601	0.0296346	33.7443	0.424972
	$\mathcal{R}$	even	1.502620398	1.22581	7.98459×10^{-9}	1.25241×10^8	0.998721
		odd	2.885601	1.69871	2.14401×10^{-6}	466416	0.999967
		even	4.13079	2.03243	0.000112761	8868.28	0.999897
		odd	5.2051	2.28147	0.00218277	458.134	0.964972
		even	6.033	2.45622	0.0300386	33.2905	0.42376
3	$\mathcal{L}$	odd	0.136755	0.369804	0.0000263936	37888	0.999961
		even	0.39192	0.626035	0.00123317	810.918	0.965227
		odd	0.607	0.779102	0.0219376	45.5838	0.365007
	$\mathcal{R}$	even	0.136763	0.369815	0.0000263447	37958.2	0.99861
		odd	0.39195	0.626059	0.00123482	809.836	0.965131
		even	0.607	0.779102	0.0221197	45.2086	0.364746
5	$\mathcal{L}$	odd	0.04936	0.222171	0.000811223	1232.71	0.965989
		even	0.1419	0.376696	0.040258	24.8398	0.245507
	$\mathcal{R}$	even	0.04937	0.222194	0.000810324	1234.07	0.966584
		odd	0.1421	0.376962	0.0439204	22.7684	0.241676
7	$\mathcal{L}$	odd	0.02423	0.15566	0.00524879	190.52	0.565059
	$\mathcal{R}$	even	0.02425	0.155724	0.00516514	193.606	0.567736
9	$\mathcal{L}$	odd	0.01331	0.115369	0.0193406	51.7047	0.313287
	$\mathcal{R}$	even	0.01325	0.115109	0.0171465	58.3209	0.322988

Table 1. The eigenvalues m^2, mass, width and lifetime of left- and right-chiral fermions with odd-parity and even-parity solutions for the coupling $F(\phi,\chi,\rho) = \phi^k\chi\rho$. $\mathcal{C}$ and $\mathcal{P}$ stand for chirality and parity, respectively. $\mathcal{L}$ and $\mathcal{R}$ are short for left-handed and right-handed, respectively. The parameters are $k = \{1,\, 3,\, 5,\, 7,\, 9\}$, $a = 0.05$ and $\eta = 1$.

2.885601, 4.13079, 5.2051, 6.033. The corresponding right-handed eigenfunctions are shown in figure 9. The configurations of figures 9(a), 9(c) and 9(e) are even-parity eigenfunctions, and the other two are odd-parity ones. This situation is the reverse of that with left-handed fermions. From the figures 8 and 9, we can also see that odd-parity eigenfunctions and even-parity eigenfunctions are placed at the five resonant peaks with irregular intervals of m. The difference is that the first resonance state is known as even-parity.

Comparing figures 5 and 6 with figures 8 and 9, respectively, we find that the nth massive resonance with left-chirality and the nth one with right-chirality have the same mass, i.e., the spectra of massive odd (even) left-handed and even (odd) right-handed fermionic resonances are the same. At the same time, excluded from the error in the numerical calculations, their lifetimes listed in table 1 are in general of the same order of magnitude. This demonstrates that it is possible to compose a Dirac fermion from a
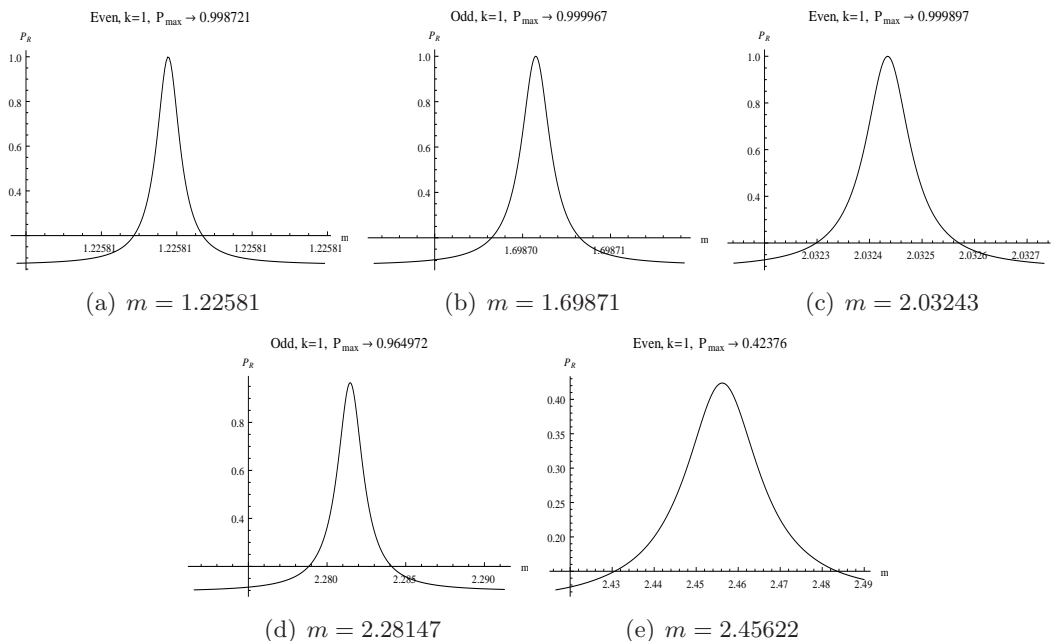
Figure 8. The probability P_R (as a function of m) for finding the even parity (upper three resonant peaks) and odd parity (under three resonant peaks) massive KK modes of the right-chiral fermions around the brane location for the coupling $F(\phi, \chi, \rho) = \phi\chi\rho$. The parameters are set to $z_{\max} = 210$, $a = 0.05$ and $\eta = 1$.

left-handed fermion with odd-parity and a right-handed one with even-parity, and vice versa. This means that the general chiral decomposition expression eq. (2.13) becomes two explicit forms

$$\Psi(x, z) = e^{-2A} \left(\sum_n \psi_{Ln}(x) f_{Ln}^{(E)}(z) + \sum_n \psi_{Rn}(x) f_{Rn}^{(O)}(z) \right) , \qquad (3.16a)$$

$$\Psi(x, z) = e^{-2A} \left(\sum_n \psi_{Ln}(x) f_{Ln}^{(O)}(z) + \sum_n \psi_{Rn}(x) f_{Rn}^{(E)}(z) \right) , \qquad (3.16b)$$

where the superscripts E and O stands for even-parity and odd-parity, respectively. We call this kind of decomposition the parity-chiral decomposition instead of the general chiral decomposition. In fact, this is not difficult to understand, because in mathematics, any function can be decomposed into an even function and an odd one. This implies that the parity and the chirality of massive fermions are conserved in a sense. We can also see that the resonance states with relatively smaller mass have a relatively longer lifetime. This conclusion is consistent with the results obtained in the single-scalar constructed dS thick brane [46].

It is worth noting that, the key point here is that we have considered two types of initial conditions (3.13) and (3.14). These two types of initial conditions lead to odd- and even-parity solutions. In fact, as mentioned in the earlier work, we found in refs. [30, 31] that the spectra of the bound massive KK modes of left- and right-chiral fermions are also the same, where the effective potentials for KK modes of fermions are modified Pöschl-Teller potentials.
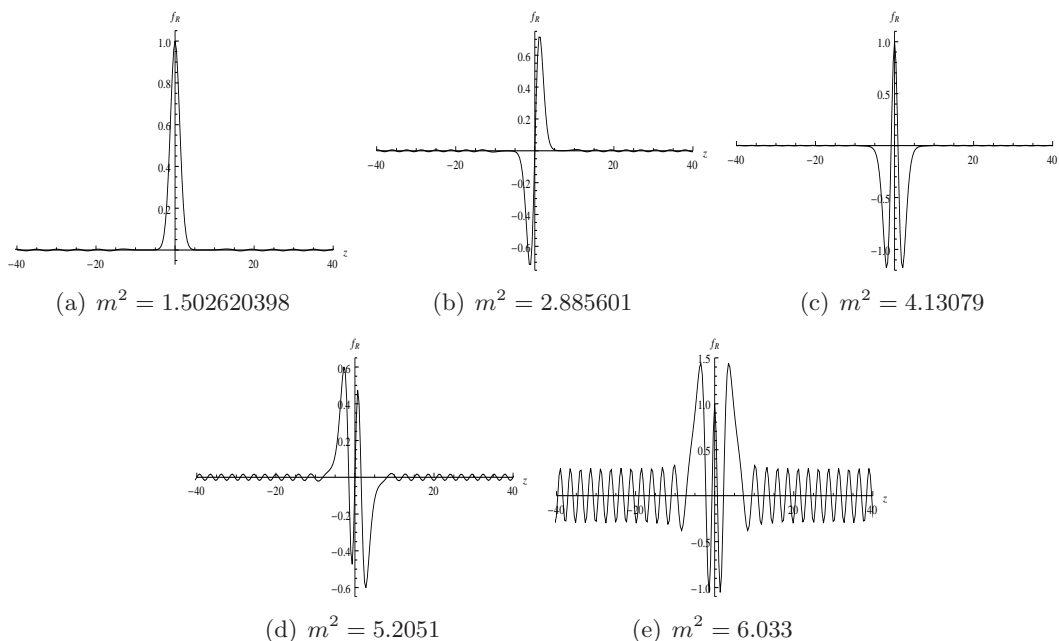
Figure 9. The shapes of the even parity (upper three) and odd parity (under three) resonance states $f_R(z)$ of right-chiral fermions for the coupling $F(\phi, \chi, \rho) = \phi\chi\rho$ with different m^2. The parameters are set to $z_{\max} = 210$, $a = 0.05$ and $\eta = 1$.

3.2 Case II: $F(\phi, \chi, \rho) = \phi^k \chi \rho$ with odd $k > 1$

Next, we consider a natural generalization of the simplest Yukawa coupling: $F(\phi, \chi, \rho) = \phi^k \chi\rho$, where k is a positive odd integer, and $k > 1$. The similar generalized couplings have been studied in refs. [46, 55]. For this coupling, the potentials for the KK modes of left- and right-handed fermions (3.7) become the form below

$$V_L(y) = \frac{2a-1}{144a^2}\eta \exp\left(\frac{2(1-3a)}{9a}\tanh^2(2ay)\right)\cosh^{-4-\frac{4}{9a}}(2ay)\tanh^{k-1}(2ay)$$
$$\times \left\{27(2a-1)\eta\tanh^{k+1}(2ay) - 16\sqrt{3}a(1+9a)\sinh^2(2ay)\right.$$
$$\left. +8\sqrt{3}a\left[9ak - (6a-2)\tanh^2(2ay)\right]\right\}, \tag{3.17a}$$
$$V_R(y) = V_L(y)|_{\eta \to -\eta}, \tag{3.17b}$$

It is easy to see that both the two potentials have a simple asymptotic behavior:

$$V_{L,R}(\pm\infty) = V_{L,R}(0) = 0. \tag{3.18}$$

The potentials cannot be expressed as explicit functions with the variable z. But by means of numerical methods, we can get the relationship between the potentials and the variable z. The graphics of the numerical potentials are depicted in figures 10 and 11 for different values of a, η and k. As mentioned in ref. [46], the potential well for left-handed fermions
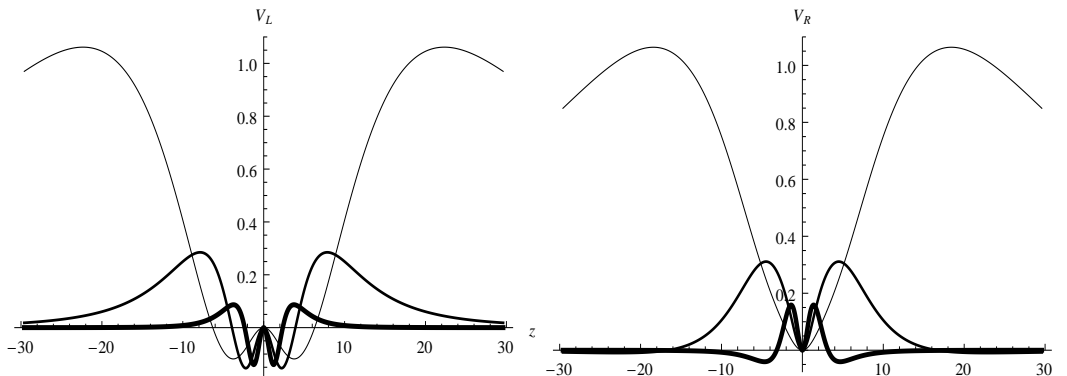
Figure 10. Potentials $V_L(z)$ and $V_R(z)$ for left- and right-handed chiral fermions with $F(\phi, \chi, \rho) = \phi^3 \chi \rho$. The parameters are set to $\eta = 1$, and $a = 0.05$ (thin trace), 0.1, 0.2 (thick trace).

becomes a double-well, while, for any positive η, there is a potential well for right-handed fermions. The lowest point of the potential well for right-handed fermions sits on the origin of the extra coordinate z. For given η and k, as a increases, the depth of the potential wells for left- and right-handed fermions will be shallower and shallower. On the other hand, for given η and a, the smaller the parameter k is, the deeper the depth of the potential wells. The third situation is that, for given a and k, the greater the absolute value of η is, the deeper the depth of the potential wells. The graphics are not drawn here.

As we know, there is a continuous gapless spectrum of KK modes for both left- and right-chiral fermions. The zero modes of left-handed fermions

$$f_{L0}(z) \propto \exp\left(-\eta \int_0^z d\bar{z} e^{A(\bar{z})} \phi^k(\bar{z}) \chi(\bar{z}) \rho(\bar{z}) \right) \tag{3.19}$$

can also not be normalized, while the following one for $F = \phi^k$ with $\eta > 2/9$ is normalizable:

$$f_{L0}(z) \propto \exp\left(-\eta \int_0^z d\bar{z} e^{A(\bar{z})} \phi^k(\bar{z}) \right). \tag{3.20}$$

The emergence of potential wells shown in figures 10 and 11 are also related to resonances. From figures 10 and 11, we see that some characteristics of these potentials are very different from those in ref. [46]. Here, for given η and a, the larger the parameter k is, the lower the depth of the potential wells. Therefore, we speculate that the number of resonance states will be reduced with the increase of k, rather than the case in ref. [46]. Next, we will prove this conjecture.

In order to study the resonance states, we consider the massive KK modes now. Just the same as the previous subsection, using the Numerov method, we will find the numerical solutions of Schrödinger equations with the purely numerical potentials (3.17) under the two types of the initial conditions (3.13) and (3.14). We first consider the case $F(\phi, \chi, \rho) = \phi^3 \chi \rho$ to see what will happen. For $a = 0.05$ and $\eta = 1$, we choose $z_{\max} = 370$. The eigenfunctions of the massive KK modes of left-handed and right-handed fermions with the even parity and odd parity are obtained with different m^2. The results of the numerical calculations are
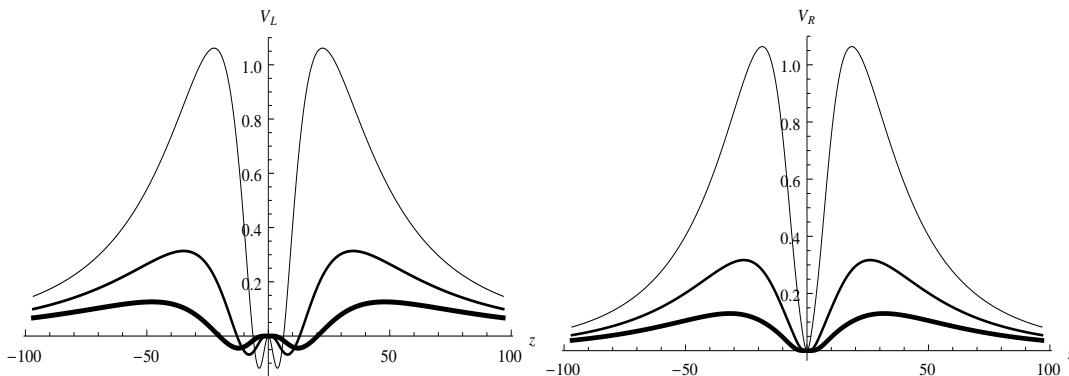
Figure 11. Potentials $V_L(z)$ and $V_R(z)$ for left- and right-handed chiral fermions with $F(\phi, \chi, \rho) = \phi^k \chi \rho$. The parameters are set to $a = 0.05$, $\eta = 1$, and $k = 3$(thin trace), 5, 7(thick trace).

plotted in figure 12. Comparing figures 6 and 9 with figure 12, we see that the number of resonances of the case $F(\phi, \chi, \rho) = \phi^3 \chi \rho$ is less than that of $F(\phi, \chi, \rho) = \phi \chi \rho$ for the same set of the parameters. This proves our previous conjecture about the number of resonances. However, if we reduce the value of a, the number of resonance states will increase. For $a = 0.01$ and $\eta = 1$, the probability for finding the massive KK modes of the left- and right-chiral fermions around the brane location are shown in figure 13. Here, we mainly discuss the number of resonance states. We can see that there have been a lot of increases of the number of the resonance states. However, because of the step size of the eigenvalue is not small enough, the probability of the resonant peaks we can see in figure 13 is not true size, and the actual probability is generally larger than that shown in the graphics.

In addition, we can investigate the other cases when k takes the following values {3, 5, 7, 9}. The eigenvalues m_n^2, mass m_n, width Γ and lifetime τ of left- and right-chiral fermions for the coupling $F(\phi, \chi, \rho) = \phi^k \chi \rho$ are also listed in table 1, here, n represents the nth-resonance state. The results show that, when k increases, the number of the resonance states gradually reduces, and when $k = 11$, the number decreases to 0. This means that, if $k \geq 11$, there would be no resonance state at all. And at the same time, there exists a finite number of resonance states for arbitrary k. These results are very different from that obtained in ref. [46], where the number of resonance states increases with k, and it is boundless for $k \to \infty$. The reason is that, for the coupling $F(\phi, \chi, \rho) = \phi^k \chi \rho$, the absolute value of the scalar field at finite z in our current case is smaller than 1. Hence, for given η and a, the larger the parameter k is, the weaker the kink-fermion coupling and so smaller the depth of the potential wells. For large enough k, there will be no resonance states because the potential wells are not deep enough.

It can be seen that, for a given $k \geq 3$, the resonances with lower mass would have longer lifetime. This is consistent with the previous result with $k = 1$. In addition, it is worth noting that, for $3 \leq k \leq 9$, all of the resonance states satisfy the parity-chiral decompositions (3.16) in a given range of error. In order to visualize the structure of resonances, we give all the mass spectrum of resonances on the thick brane with the
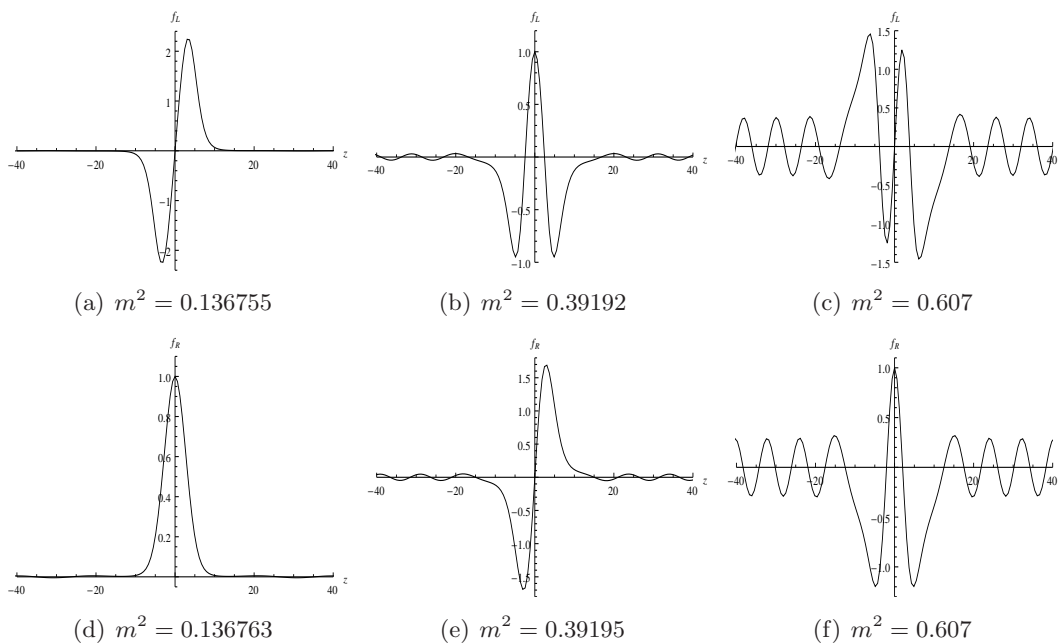
Figure 12. The shapes of massive KK modes of left-handed (upper) and right-handed (under) fermions with the even parity and odd parity for the coupling $F(\phi, \chi, \rho) = \phi^k \chi \rho$ with different m^2. The parameters are set to $k = 3$, $z_{\max} = 370$, $a = 0.05$, and $\eta = 1$.
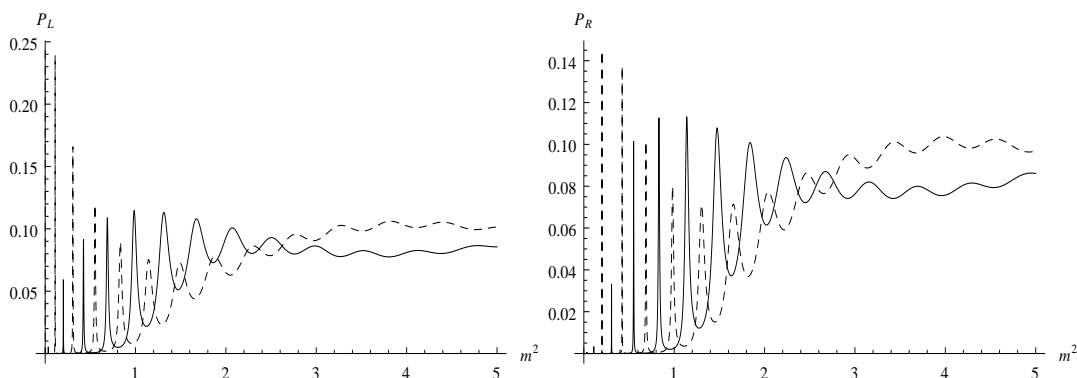
Figure 13. The probability $P_{L,R}$ (as a function of m^2) for finding massive KK modes of left- and right-chiral fermions with mass m^2 around the brane location for the coupling $F(\phi, \chi, \rho) = \phi^3 \chi \rho$. Solid lines and dashed lines are plotted for the odd-parity and even-parity massive fermions, respectively. The parameters are $a = 0.01$ and $\eta = 1$.

coupling $F(\phi, \chi, \rho) = \phi^k \chi \rho$ for $k = 1, 3, 5, 7, 9$ in figure 14. It turns out that, for each eigenvalue m_n^2, we get a pair of resonance states. They always appear at the same time, and have opposite parity and chiral. Remarkably, the first state of the resonance spectrum with lower k would have a relatively larger mass m_1. For a given k, as n increases, the mass gap $\Delta m = m_n - m_{n-1}$ of the resonances is getting smaller and smaller.

Figure 14. Mass spectra of resonances for the coupling $F(\phi, \chi, \rho) = \phi^k \chi \rho$. The parameters are set to $k = \{1, 3, 5, 7, 9\}$, $a = 0.05$ and $\eta = 1$.

4 Resonances on a Bloch brane model

In this section, we re-analysis the problems of resonances in a Bloch brane model [49] with the coupling $F(\phi, \chi) = \phi \chi$ considered in [45] and clarify some small issues. By applying the previous method, we further investigate the number and the lifetime of the resonances in the two-scalar generated Bloch brane with the coupling $F(\phi, \chi) = \phi^k \chi$, $k = 3, 5, 7, 9$. Finally, we give all the mass spectrum of the models.
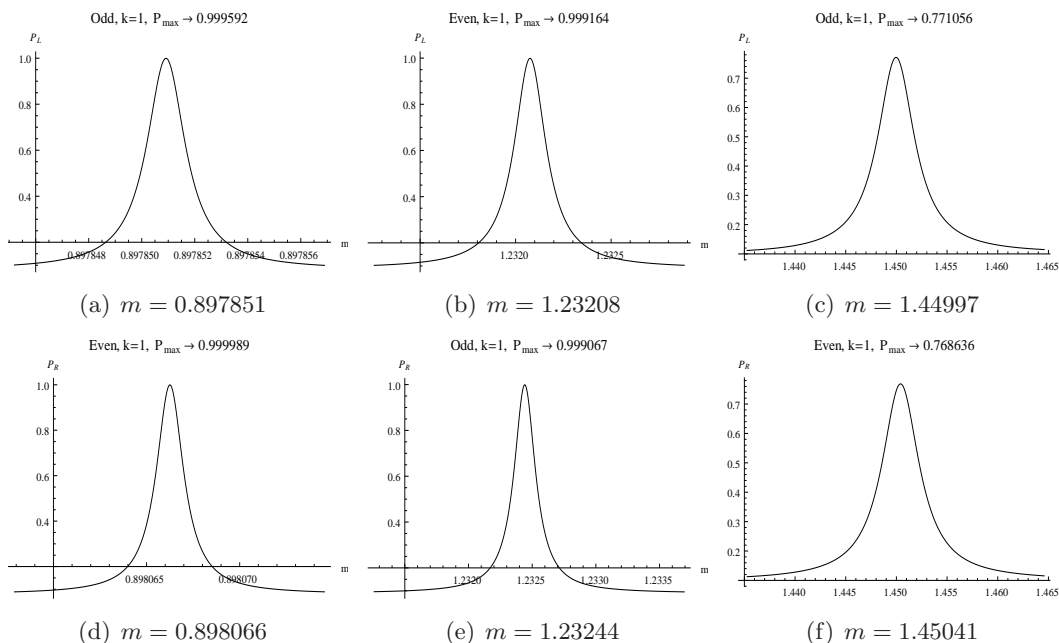
Figure 15. The probability $P_{L,R}$ (as a function of m) for finding the even-parity and odd-parity massive KK modes of the left- and right-chiral fermions around the Bloch brane [49] location for the coupling $F(\phi, \chi) = \phi\chi$. Part of the results have been given in ref. [45]. The parameters are set to $z_{\max} = 200$, $a = 0.05$, $\eta = 1$.

4.1 Case I: $F(\phi, \chi) = \phi^k \chi$ with $k = 1$

In ref. [45], the simplest Yukawa coupling $\overline{\Psi}\phi\chi\Psi$ between two scalar fields and a spinor field was investigated for a two-scalar generated Bloch brane model [49]. The fermionic resonance states for both chiralities were discussed, and their appearance is related to the internal structure of the brane. Here, in order to facilitate the discussion, we recast the kink-fermion coupling $\overline{\Psi}\phi\chi\Psi$ into $\overline{\Psi}F(\phi, \chi)\Psi$ with $F(\phi, \chi) = \phi^k \chi$ and $k = 1$.

By using the Numerov method, we solve the Schrödinger equation for the massive KK modes and obtain a series of resonances. For $a = 0.05$ and $\eta = 1$, we choose $z_{\max} = 200$. The probability for finding the even parity and odd parity massive KK modes of the left- and right-chiral fermions around the Bloch brane location are shown in figure 15. We found a total of three resonant peaks and their eigenvalues m^2 are in the potential well below the maximum. It is worth noting that the number of the resonance states we discussed here is a physical quantity which has not been well defined. The number of the resonance states we are talking about here are the sum of the resonance states whose energy eigenvalues are lower than the highest point of the potential wells. The massive KK modes whose eigenvalues m^2 are very close to or higher than the highest point of the potential wells may also have a a little resonance, but because the probability of these resonance states are generally very small and they have quite a little lifetime, so we do not take into account them.

The shapes of the corresponding massive KK modes of left- and right-handed fermions with the even parity and odd parity for Bloch brane with different m^2 are shown in figure 16.
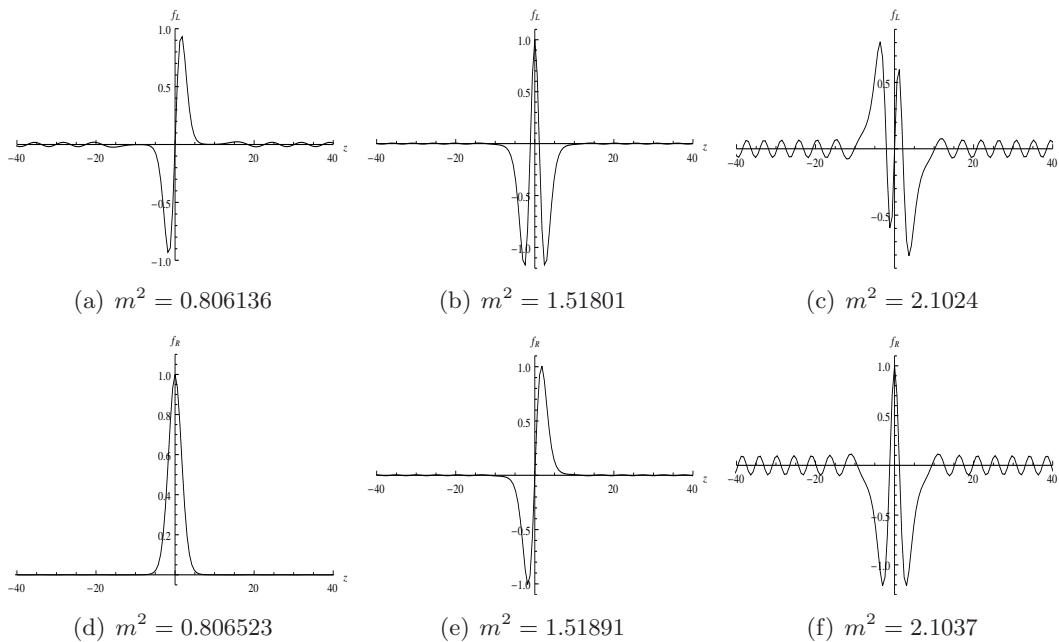
Figure 16. The shapes of resonances on the Bloch brane for the coupling $F(\phi, \chi) = \phi\chi$. The parameters are set to $z_{\max} = 200$, $a = 0.05$, $\eta = 1$.

There are a total of three odd-parity solutions and three even-parity solutions, on the other hand, three left-handed solutions and three right-handed solutions. This comply with the parity-chiral decomposition expression (3.16).

4.2 Case II: $F(\phi, \chi) = \phi^k \chi$ with odd $k > 1$

In this subsection, we extend the analysis to the situation $k > 1$. Use the same method, for $k = 3, 5, 7, 9$, the eigenvalues m_n^2, mass m_n, width Γ and lifetime τ for the resonances are listed in table 2. For given a and η, as k increases, the number of resonance states reduces to zero quickly. The parity-chiral decomposition expression (3.16) holds good for every k. The graphic of the mass spectrum of resonances for the coupling $F(\phi, \chi, \rho) = \phi^k \chi$ ($1 \leq k \leq 9$) is depicted in figure 17.

5 Discussion and conclusion

In this paper, we first investigated the thick branes generated from multi-scalar (especially three-scalar) fields. Then, we studied the localization and the resonances on the three-scalar and two-scalar generated branes. Using the Numerov method, we solved the Schrödinger equations for KK modes of fermions with the numerical potentials under two types of initial value conditions, which lead to the odd- and even-parity solutions. We got the wave functions of the resonance states and used them to calculate the probability and the lifetime of resonance states.

For the three-field model, we considered the generalized Yukawa coupling $\eta \overline{\Psi} \phi^k \chi \rho \Psi$ on the thick brane, where η is an arbitrary positive coupling constant and k is an odd

k	$\mathcal{C}$	$\mathcal{P}$	m_n^2	m_n	Γ	τ	$P_{\max}$
1	$\mathcal{L}$	odd	0.806136	0.897851	1.92489×10^{-6}	519510	0.999592
		even	1.51801	1.23208	0.000221484	4515	0.999164
		odd	2.1024	1.44997	0.00512333	195.186	0.771056
	$\mathcal{R}$	even	0.806523	0.898066	1.92954×10^{-6}	518260	0.999989
		odd	1.51891	1.23244	0.000223108	4482.13	0.999067
		even	2.1037	1.45041	0.00517988	193.055	0.768636
3	$\mathcal{L}$	odd	0.096964	0.31139	0.0000873266	11451.3	0.999515
		even	0.26526	0.515034	0.0048577	205.859	0.646296
	$\mathcal{R}$	even	0.096982	0.311419	0.0000884991	11299.5	0.999304
		odd	0.2653	0.515073	0.00487788	205.007	0.646222
5	$\mathcal{L}$	odd	0.03794	0.194782	0.000837101	1194.6	0.929206
	$\mathcal{R}$	even	0.03795	0.194808	0.000833316	1200.03	0.929414
7	$\mathcal{L}$	odd	0.01956	0.139857	0.00383873	260.502	0.477145
	$\mathcal{R}$	even	0.01957	0.139893	0.00373923	267.435	0.479078
9	$\mathcal{L}$	odd	0.0112	0.10583	0.015039	66.4936	0.265202
	$\mathcal{R}$	even	0.0112	0.10583	0.0135679	73.7035	0.270337

**Table 2**. The eigenvalues m^2, mass, width and lifetime for resonances of left- and right-chiral fermions with odd-parity and even-parity solutions for the coupling $F(\phi, \chi) = \phi^k \chi$. $\mathcal{C}$ and $\mathcal{P}$ stand for chirality and parity, respectively. $\mathcal{L}$ and $\mathcal{R}$ are short for left-handed and right-handed, respectively. The parameters are $a = 0.05$, $k = \{1, 3, 5, 7, 9\}$ and $\eta = 1$.

positive integer. For the two-field model, we considered the coupling $\eta\overline{\Psi}\phi^k\chi\Psi$, where the case of $k = 1$ was considered in [45]. In these models, there is a real parameter a, whose role is regulating the structure of the thick branes. The results show that the behavior of the resonances completely decided by the structure of the branes and the coupling with scalars. For a certain k, the coupling constant η and the parameter a decide the shape of the potentials and wave functions.

For $k = 1$ in the three-field model, the potential of the KK modes of left chiral fermions V_L is a modified volcano type potential. While the shape for the right one V_R is decided by a and η. For small a and large η, the potential V_R will have a potential well. When the depth of the potential well is deep enough, it will be able to trap the fermions in some sense. We obtained a series of quasibound states or the metastable states with finite lifetimes. The eigenvalues m_n^2 of the resonances were also given.

For $k > 1$ in the two-field and three-field models, the potential well for left-handed fermions becomes a double-well, which is consistent with the result obtained in ref. [46]. However, for given a and η, the number of the resonant states in these two models decreases with k. This is opposite to the result given in ref. [46] for the single-scalar generated brane case. The reason is that the absolute value of the kink ϕ in current models is less than 1, and so, when k increases, the strength of the coupling decreases.

We find that the n-th resonance of left-handed fermions with odd parity and the n-th resonance of right-handed fermions with even parity have the same mass and lifetime, and
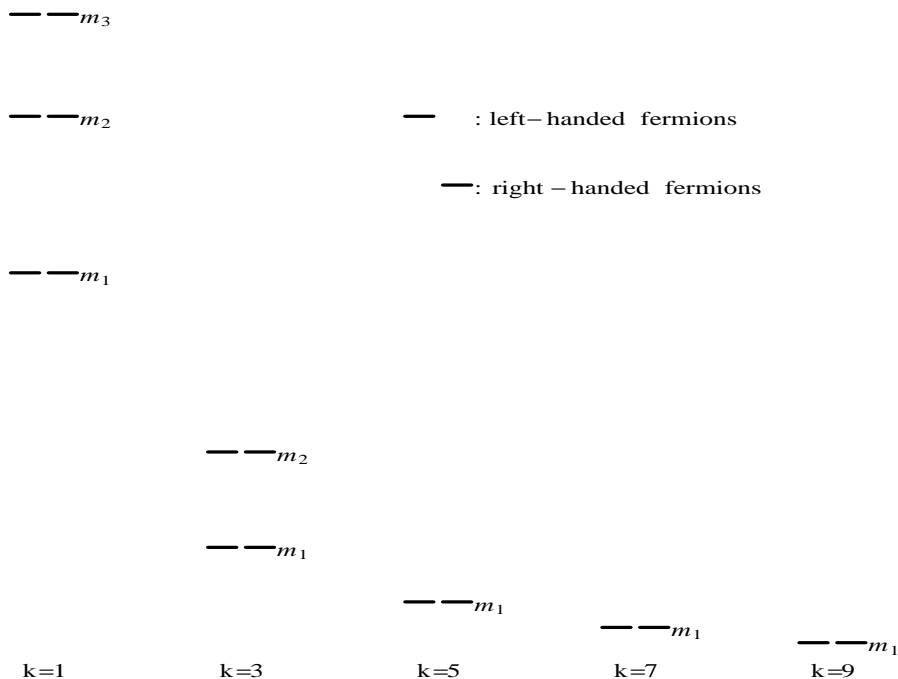
Figure 17. Mass spectrum of resonances for the coupling $F(\phi, \chi, \rho) = \phi^k \chi$. The parameters are $k = \{1, 3, 5, 7, 9\}$, $a = 0.05$ and $\eta = 1$.

vice versa. This demonstrates that it is possible to compose a Dirac fermion from the left and right KK modes [46]. However, in both chiral fermions, the parity is opposite. We call this phenomenon as the parity-chiral decomposition, and it is the explicit form of the general KK chiral decomposition of the Dirac fermions.

In our numerical calculations, for those KK modes with m^2 much larger than the maximum of the corresponding potential, they would be approximately plane waves and the probabilities for them would trend to 0.1, where we chose $z_{\text{max}} = 10z_b$ to calculate the relative probabilities. For the KK modes with m_2 close to but larger than the maximum of the potential, the probabilities for finding them around the brane P is quite small. For the sake of clarity, we give the definition of the number of the resonant states: the number of these resonant states with eigenvalue m^2 lower than the highest point of the potential. We also took into account the impact of the numerical precision. Besides, the probabilities P for the resonances are affected by z_b. So z_b cannot be too small. The resonances in other thick brane models with different kink-fermion couplings could be considered, we will propose the corresponding work on this subject in a near future.

Acknowledgments

References

[1] K. Akama, *An early proposal of "brane world"*, *Lect. Notes Phys.* **176** (1982) 267 [`hep-th/0001113`] [SPIRES].

[2] K. Akama, *Proceedings of the symposium on gauge theory and gravitation*, Nara Japan, K. Kikkawa, N. Nakanishi and H. Nariai eds., Springer-Verlag, Germany (1983).

[3] V.A. Rubakov and M.E. Shaposhnikov, *Do we live inside a domain wall?*, *Phys. Lett.* **B 125** (1983) 136 [SPIRES].

[4] V.A. Rubakov and M.E. Shaposhnikov, *Extra space-time dimensions: towards a solution to the cosmological constant problem*, *Phys. Lett.* **B 125** (1983) 139 [SPIRES].

[5] M. Visser, *An exotic class of Kaluza-Klein models*, *Phys. Lett.* **B 159** (1985) 22 [`hep-th/9910093`] [SPIRES].

[6] S. Randjbar-Daemi and C. Wetterich, *Kaluza-Klein solutions with noncompact internal spaces*, *Phys. Lett.* **B 166** (1986) 65 [SPIRES].

[7] I. Antoniadis, *A possible new dimension at a few TeV*, *Phys. Lett.* **B 246** (1990) 377 [SPIRES].

[8] N. Arkani-Hamed, S. Dimopoulos and G.R. Dvali, *The hierarchy problem and new dimensions at a millimeter*, *Phys. Lett.* **B 429** (1998) 263 [`hep-ph/9803315`] [SPIRES]; I. Antoniadis, N. Arkani-Hamed, S. Dimopoulos and G.R. Dvali, *New dimensions at a millimeter to a Fermi and superstrings at a TeV*, *Phys. Lett.* **B 436** (1998) 257 [`hep-ph/9804398`] [SPIRES].

[9] L. Randall and R. Sundrum, *A large mass hierarchy from a small extra dimension*, *Phys. Rev. Lett.* **83** (1999) 3370 [`hep-ph/9905221`] [SPIRES].

[10] L. Randall and R. Sundrum, *An alternative to compactification*, *Phys. Rev. Lett.* **83** (1999) 4690 [`hep-th/9906064`] [SPIRES].

[11] N. Arkani-Hamed, S. Dimopoulos, G.R. Dvali and N. Kaloper, *Infinitely large new dimensions*, *Phys. Rev. Lett.* **84** (2000) 586 [`hep-th/9907209`] [SPIRES].

[12] J.D. Lykken and L. Randall, *The shape of gravity*, *JHEP* **06** (2000) 014 [`hep-th/9908076`] [SPIRES].

[13] A. Kehagias, *A conical tear drop as a vacuum-energy drain for the solution of the cosmological constant problem*, *Phys. Lett.* **B 600** (2004) 133 [`hep-th/0406025`] [SPIRES].

[14] O. DeWolfe, D.Z. Freedman, S.S. Gubser and A. Karch, *Modeling the fifth dimension with scalars and gravity*, *Phys. Rev.* **D 62** (2000) 046008 [`hep-th/9909134`] [SPIRES].

[15] M. Gremm, *Four-dimensional gravity on a thick domain wall*, *Phys. Lett.* **B 478** (2000) 434 [`hep-th/9912060`] [SPIRES].

[16] M. Gremm, *Thick domain walls and singular spaces*, *Phys. Rev.* **D 62** (2000) 044017 [`hep-th/0002040`] [SPIRES]; K. Ghoroku and M. Yahiro, *Instability of thick brane worlds*, `hep-th/0305150` [SPIRES]; A. Kehagias and K. Tamvakis, *A self-tuning solution of the cosmological constant problem*, *Mod. Phys. Lett.* **A 17** (2002) 1767 [`hep-th/0011006`] [SPIRES]; *Localized gravitons, gauge bosons and chiral fermions in smooth spaces generated by a bounce*, *Phys. Lett.* **B 504** (2001) 38 [`hep-th/0010112`] [SPIRES];

M. Giovannini, *Gauge-invariant fluctuations of scalar branes*, *Phys. Rev.* **D 64** (2001) 064023 [hep-th/0106041] [SPIRES]; *Localization of metric fluctuations on scalar branes*, *Phys. Rev.* **D 65** (2002) 064008 [hep-th/0106131] [SPIRES]; S. Kobayashi, K. Koyama and J. Soda, *Thick brane worlds and their stability*, *Phys. Rev.* **D 65** (2002) 064014 [hep-th/0107025] [SPIRES].

[17] C. Csáki, J. Erlich, T.J. Hollowood and Y. Shirman, *Universal aspects of gravity localized on thick branes*, *Nucl. Phys.* **B 581** (2000) 309 [hep-th/0001033] [SPIRES].

[18] A. Campos, *Critical phenomena of thick branes in warped spacetimes*, *Phys. Rev. Lett.* **88** (2002) 141602 [hep-th/0111207] [SPIRES].

[19] A. Wang, *Thick de Sitter brane worlds, dynamic black holes and localization of gravity*, *Phys. Rev.* **D 66** (2002) 024024 [hep-th/0201051] [SPIRES].

[20] A. Melfo, N. Pantoja and A. Skirzewski, *Thick domain wall spacetimes with and without reflection symmetry*, *Phys. Rev.* **D 67** (2003) 105003 [gr-qc/0211081] [SPIRES]; K.A. Bronnikov and B.E. Meierovich, *A general thick brane supported by a scalar field*, *Grav. Cosmol.* **9** (2003) 313 [gr-qc/0402030] [SPIRES]; O. Castillo-Felisola, A. Melfo, N. Pantoja and A. Ramirez, *Localizing gravity on exotic thick 3-branes*, *Phys. Rev.* **D 70** (2004) 104029 [hep-th/0404083] [SPIRES]; M. Minamitsuji, W. Naylor and M. Sasaki, *Quantum fluctuations on a thick de Sitter brane*, *Nucl. Phys.* **B 737** (2006) 121 [hep-th/0508093] [SPIRES].

[21] R. Guerrero, A. Melfo and N. Pantoja, *Self-gravitating domain walls and the thin-wall limit*, *Phys. Rev.* **D 65** (2002) 125010 [gr-qc/0202011] [SPIRES].

[22] V. Dzhunushaliev, V. Folomeev, D. Singleton and S. Aguilar-Rudametkin, *6D thick branes from interacting scalar fields*, *Phys. Rev.* **D 77** (2008) 044006 [hep-th/0703043] [SPIRES]; V. Dzhunushaliev, V. Folomeev, K. Myrzakulov and R. Myrzakulov, *Thick brane in 7D and 8D spacetimes*, *Gen. Rel. Grav.* **41** (2009) 131 [arXiv:0705.4014] [SPIRES].

[23] D. Bazeia, F.A. Brito and J.R.S. Nascimento, *Supergravity brane worlds and tachyon potentials*, *Phys. Rev.* **D 68** (2003) 085007 [hep-th/0306284] [SPIRES]; D. Bazeia, C. Furtado and A.R. Gomes, *Brane structure from scalar field in warped spacetime*, *JCAP* **02** (2004) 002 [hep-th/0308034] [SPIRES]; D. Bazeia, F.A. Brito and A.R. Gomes, *Locally localized gravity and geometric transitions*, *JHEP* **11** (2004) 070 [hep-th/0411088] [SPIRES]; D. Bazeia, F.A. Brito and L. Losano, *Scalar fields, bent branes and RG flow*, *JHEP* **11** (2006) 064 [hep-th/0610233] [SPIRES].

[24] Y. Shtanov, V. Sahni, A. Shafieloo and A. Toporensky, *Induced cosmological constant and other features of asymmetric brane embedding*, *JCAP* **04** (2009) 023 [arXiv:0901.3074] [SPIRES]; K. Farakos, N.E. Mavromatos and P. Pasipoularides, *Asymmetrically warped brane models, bulk photons and Lorentz invariance*, arXiv:0902.1243 [SPIRES]; M. Sarrazin and F. Petit, *Equivalence between domain-walls and "non-commutative" two-sheeted spacetimes. Model-independent matter swapping between branes*, arXiv:0903.2498 [SPIRES]; V. Dzhunushaliev, V. Folomeev and M. Minamitsuji, *Thick de Sitter brane solutions in higher dimensions*, *Phys. Rev.* **D 79** (2009) 024001 [arXiv:0809.4076] [SPIRES]; Y.X. Liu, Y. Zhong and K. Yang, *Warped thick brane solutions of scalar fields with generalized dynamics*, arXiv:0907.1952 [SPIRES].

[25] W.D. Goldberger and M.B. Wise, *Modulus stabilization with bulk fields*, *Phys. Rev. Lett.* **83** (1999) 4922 [`hep-ph/9907447`] [SPIRES].

[26] V. Dzhunushaliev, V. Folomeev and M. Minamitsuji, *Thick brane solutions*, `arXiv:0904.1775` [SPIRES].

[27] C. Ringeval, P. Peter and J.P. Uzan, *Localization of massive fermions on the brane*, *Phys. Rev.* **D 65** (2002) 044016 [`hep-th/0109194`] [SPIRES].

[28] T.R. Slatyer and R.R. Volkas, *Cosmology and fermion confinement in a scalar-field-generated domain wall brane in five dimensions*, *JHEP* **04** (2007) 062 [`hep-ph/0609003`] [SPIRES].

[29] Y.-X. Liu, X.-H. Zhang, L.-D. Zhang and Y.-S. Duan, *Localization of matters on pure geometrical thick branes*, *JHEP* **02** (2008) 067 [`arXiv:0708.0065`] [SPIRES].

[30] Y.-X. Liu, L.-D. Zhang, S.-W. Wei and Y.-S. Duan, *Localization and mass spectrum of matters on Weyl thick branes*, *JHEP* **08** (2008) 041 [`arXiv:0803.0098`] [SPIRES].

[31] Y.-X. Liu, Z.-H. Zhao, S.-W. Wei and Y.-S. Duan, *Bulk matters on symmetric and asymmetric de Sitter thick branes*, *JCAP* **02** (2009) 003 [`arXiv:0901.0782`] [SPIRES].

[32] S.L. Parameswaran, S. Randjbar-Daemi and A. Salvio, *Gauge fields, fermions and mass gaps in* $6D$ *brane worlds*, *Nucl. Phys.* **B 767** (2007) 54 [`hep-th/0608074`] [SPIRES].

[33] Y.X. Liu, L. Zhao and Y.S. Duan, *Localization of Fermions on a string-like defect*, *JHEP* **04** (2007) 097 [`hep-th/0701010`] [SPIRES];
L. Zhao, Y.-X. Liu and Y.-S. Duan, *Fermions in gravity and gauge backgrounds on a brane world*, *Mod. Phys. Lett.* **A 23** (2008) 1129 [`arXiv:0709.1520`] [SPIRES].

[34] G. De Pol, H. Singh and M. Tonin, *Action with manifest duality for maximally supersymmetric six-dimensional supergravity*, *Int. J. Mod. Phys.* **A 15** (2000) 4447 [`hep-th/0003106`] [SPIRES].

[35] Y.-X. Liu, L. Zhao, X.-H. Zhang and Y.-S. Duan, *Fermions in self-dual vortex background on a string-like defect*, *Nucl. Phys.* **B 785** (2007) 234 [`arXiv:0704.2812`] [SPIRES].

[36] Y.-Q. Wang, T.-Y. Si, Y.-X. Liu and Y.-S. Duan, *Fermionic zero modes in self-dual vortex background*, *Mod. Phys. Lett.* **A 20** (2005) 3045 [`hep-th/0508111`] [SPIRES];
Y.-S. Duan, Y.-X. Liu and Y.-Q. Wang, *Fermionic zero modes in gauge and gravity backgrounds on* T^2, *Mod. Phys. Lett.* **A 21** (2006) 2019 [`hep-th/0602157`] [SPIRES];
Y.X. Liu, Y.S. Duan and Y.Q. Wang, *Fermionic zero modes in self-dual vortex background on a torus*, *Commun. Theor. Phys.* **48** (2007) 675 [SPIRES].

[37] R.S. Torrealba S., *Exact Abelian Higgs vortices as* $6D$ *brane worlds*, `arXiv:0803.0313` [SPIRES].

[38] G. Starkman, D. Stojkovic and T. VachasPati, *Zero modes of fermions with a general mass matrix*, *Phys. Rev.* **D 65** (2002) 065003 [`hep-th/0103039`] [SPIRES]; *Neutrino zero modes on electroweak strings*, *Phys. Rev.* **D 63** (2001) 085011 [`hep-ph/0007071`] [SPIRES];
D. Stojkovic, *Fermionic zero modes on domain walls*, *Phys. Rev.* **D 63** (2001) 025010 [`hep-ph/0007343`] [SPIRES].

[39] S. Randjbar-Daemi and M.E. Shaposhnikov, *Fermion zero-modes on brane-worlds*, *Phys. Lett.* **B 492** (2000) 361 [`hep-th/0008079`] [SPIRES].

[40] N. Barbosa-Cendejas, A. Herrera-Aguilar, M.A. Reyes Santos and C. Schubert, *Mass gap for gravity localized on Weyl thick branes*, *Phys. Rev.* **D 77** (2008) 126013 [`arXiv:0709.3552`] [SPIRES];

N. Barbosa-Cendejas, A. Herrera-Aguilar, U. Nucamendi and I. Quiros, *Mass hierarchy and mass gap on thick branes with Poincaré symmetry*, arXiv:0712.3098 [SPIRES].

[41] Y.X. Liu, L.D. Zhang, L.J. Zhang and Y.S. Duan, *Fermions on thick branes in background of sine-Gordon kinks*, *Phys. Rev.* **D 78** (2008) 065025 [arXiv:0804.4553] [SPIRES].

[42] Y. Kodama, K. Kokubu and N. Sawado, *Localization of massive fermions on the baby-skyrmion branes in 6 dimensions*, arXiv:0812.2638 [SPIRES];
Y. Brihaye and T. Delsate, *Remarks on bell-shaped lumps: stability and fermionic modes*, *Phys. Rev.* **D 78** (2008) 025014 [arXiv:0803.1458] [SPIRES].

[43] D. Bazeia, F.A. Brito and R.C. Fonseca, *Fermion states on domain wall junctions and the flavor number*, *Eur. Phys. J.* **C 63** (2009) 163 [arXiv:0809.3048] [SPIRES];
P. Koroteev and M. Libanov, *Spectra of field fluctuations in braneworld models with broken bulk Lorentz invariance*, *Phys. Rev.* **D 79** (2009) 045023 [arXiv:0901.4347] [SPIRES];
A. Flachi and M. Minamitsuji, *Field localization on a brane intersection in anti-de Sitter spacetime*, *Phys. Rev.* **D 79** (2009) 104021 [arXiv:0903.0133] [SPIRES].

[44] D. Bazeia, A.R. Gomes and L. Losano, *Gravity localization on thick branes: a numerical approach*, *Int. J. Mod. Phys.* **A 24** (2009) 1135 [arXiv:0708.3530] [SPIRES].

[45] C.A.S. Almeida, J. Ferreira, M. M., A.R. Gomes and R. Casana, *Fermion localization and resonances on two-field thick branes*, *Phys. Rev.* **D 79** (2009) 125022 [arXiv:0901.3543] [SPIRES].

[46] Y.-X. Liu, J. Yang, Z.-H. Zhao, C.-E. Fu and Y.-S. Duan, *Fermion localization and resonances on a de Sitter thick brane*, *Phys. Rev.* **D 80** (2009) 065019 [arXiv:0904.1785] [SPIRES].

[47] M. Cvetič and M. Robnik, *Gravity trapping on a finite thickness domain wall: an analytic study*, *Phys. Rev.* **D 77** (2008) 124003 [arXiv:0801.0801] [SPIRES].

[48] D. Bazeia, L. Losano and C. Wotzasek, *Domain walls in three-field models*, *Phys. Rev.* **D 66** (2002) 105025 [hep-th/0206031] [SPIRES].

[49] D. Bazeia and A.R. Gomes, *Bloch brane*, *JHEP* **05** (2004) 012 [hep-th/0403141] [SPIRES].

[50] V. Dzhunushaliev, H.-J. Schmidt, K. Myrzakulov and R. Myrzakulov, *Thick brane solution with two scalar fields*, in proceedings of *11th M. Grossmann meeting, 2008*, part B, pg. 1210–1212, gr-qc/0610100 [SPIRES].

[51] A. Alonso Izquierdo, M.A. Gonzalez Leon and J. Mateos Guilarte, *Stability of kink defects in a deformed $O(3)$ linear σ-model*, math-ph/0204041 [SPIRES].

[52] B.V. Numerov, *A method of extrapolation of perturbations*, *Roy. Ast. Soc. Monthly Notices* **84** (1924) 592;
M. Mueller and H. Huber, *Solution of the 1-D Schrödinger equation*, http://www.maplesoft.com/applications/view.aspx?SID=3828.

[53] D. Bazeia, A.R. Gomes and L. Losano, *Gravity localization on thick branes: a numerical approach*, *Int. J. Mod. Phys.* **A 24** (2009) 1135 [arXiv:0708.3530] [SPIRES].

[54] R. Gregory, V.A. Rubakov and S.M. Sibiryakov, *Opening up extra dimensions at ultra-large scales*, *Phys. Rev. Lett.* **84** (2000) 5928 [hep-th/0002072] [SPIRES].

[55] Y.-X. Liu, C.-E. Fu, L. Zhao and Y.-S. Duan, *Localization and mass spectra of fermions on symmetric and asymmetric thick branes*, *Phys. Rev.* **D 80** (2009) 065020 [arXiv:0907.0910] [SPIRES].